

New Instruments and Measurement Methods

MEASUREMENT OF FOURIER SPECTRA OF TWO-DIMENSIONAL FUNCTIONS

N. S. SHESTOV,* E. O. FEDOROVA, V. F. ZAKHARENKO, and N. A. STAVITSKAYA

Usp. Fiz. Nauk 96, 717-740 (December, 1968)

I. INTRODUCTION

THE solution of many theoretical and practical problems in optics, radio engineering, communication theory, detection theory, and many branches of science and technology is based on the use of Fourier-analysis methods. Among the various applications of these methods, we can single out a large group of problems connected with the need of analyzing two-dimensional functions.

In optics, two-dimensional Fourier transforms are used to explain theoretically processes of image formation, image transmission, and methods of acting on images^[1-3]. The transformation formulas make it possible, for example, to represent in mathematical form the diffraction phenomena with the aid of which image theory is constructed, namely to establish the analytic connection between the distribution of the amplitudes of the optical oscillations on the pupils and the distribution of the amplitudes in the image. The existence of such a connection uncovers wide possibilities for apodization—acting on an image by varying the amplitude distribution on the pupil^[4].

The study of the apodizing action of various diaphragms, filters with variable transmission, and other devices that limit the pupil, reduces to the determination of the distribution of the amplitudes in the diffraction image. This problem, as well as the inverse problem, namely the determination of the form of the apodizing filter for a specified diffraction pattern, is solved with the aid of the direct and inverse Fourier transformations. Similar problems are solved in radio engineering, when the form of the directivity pattern of an antenna is determined for a specified distribution of the currents in the antenna aperture, or the current distribution is determined from a specified directivity pattern^[5].

Two-dimensional Fourier transforms are very useful in the analysis of the formation of images of extended objects^[3]. In this case one uses the transformation property, according to which the transform of a function describing the distribution of the illumination in the image is equal to the product of the transforms of the functions characterizing the brightness of the object and the scattering spots of the optical system.

Fourier analysis is used extensively in the design of optimal optical detection systems^[6,7]. In this case it is necessary to know the space-frequency Fourier spectra of the objects to be detected, and the energy space-frequency spectra of the random field of brightness distribution, against the background of which the detection is carried out. Data on the space-frequency

spectra of images of symbols and figures are used to develop image recognition systems.^[8]

In television, spectral analysis of the images is used to determine the frequency and statistical characteristics of television signals^[9-11].

Finally, new methods for estimating photographic systems are based on the use of so-called "frequency-contrast characteristics," which are also determined with the aid of Fourier transforms^[12].

This list can be continued, but it suffices to explain the recent increased interest in the development of apparatus methods for obtaining two-dimensional Fourier transforms.

To obtain two-dimensional Fourier transforms in any of the aforementioned problems, it is necessary to be able to evaluate, by one method or another, two-dimensional integrals of the form

$$f(P, Q) = \iint_{(S)} f(X, Y) e^{-i(PX+QY)} dX dY, \quad (1)$$

where $f(X, Y)$ is a real function of the coordinates X and Y , specified on the area S . In the case when X and Y are spatial coordinates, the function $f(P, Q)$ is called the two-dimensional space-frequency spectrum of the Fourier function $f(X, Y)$, and P and Q are the spatial wave numbers corresponding to the axes X and Y . The function $f(P, Q)$ is complex, since it contains information on the phase shifts of the individual harmonic components relative to a point inside S , chosen to be the origin. Expanding in (1) the exponential factor in accordance with Euler's formula, we can represent $f(P, Q)$ in the form of an exponential function:

$$f(P, Q) = |f(P, Q)| e^{i\varphi(P, Q)}, \quad (2)$$

where the modulus of the spectrum is

$$|f(P, Q)| = \sqrt{J_{\cos}^2(P, Q) + J_{\sin}^2(P, Q)}, \quad (3)$$

the argument (phase) of the spectrum is

$$\varphi(P, Q) = -\operatorname{arctg} \frac{J_{\sin}(P, Q)}{J_{\cos}(P, Q)}, \quad (4)$$

and in turn the cosine component of the Fourier expansion is

$$J_{\cos}(P, Q) = \iint_{(S)} f(X, Y) \cos(PX + QY) dX dY \quad (5)$$

and the sine component is

$$J_{\sin}(P, Q) = \iint_{(S)} f(X, Y) \sin(PX + QY) dX dY. \quad (6)$$

In some problems it is necessary to calculate the square of the Fourier spectrum

$$|f(P, Q)|^2 = f(P, Q) f^*(P, Q) = |f(P, Q)|^2; \quad (7)$$

Here $f^*(P, Q)$ denotes the function conjugate to $f(P, Q)$. In this case the information concerning the phase is lost.

*Deceased.

The two-dimensional spectrum $f(P, Q)$ can be determined analytically from the specified function $f(X, Y)$ by simple means only if the latter can be approximated by a product of sufficiently simple functions that depend on a single coordinate; for functions of arbitrarily complex form, and all the more when $f(X, Y)$ represents a random field, the calculation of the spectrum $f(P, Q)$, even with the aid of electronic computers, entails great difficulties or becomes impossible. At the same time, this problem can be solved relatively simply with the aid of optical-electronic devices that analyze the photographic images of two-dimensional functions. Optical systems, by their very nature, have two degrees of freedom (this is their main advantage over electronic systems, which have only one degree of freedom), and therefore make it possible to integrate simultaneously with respect to two variables, i.e., with respect to an area.

An example of an optical system that realizes a two-dimensional Fourier transform is the setup for the observation of Fraunhofer diffraction^[3,13], consisting of a coherent-light source, a collimator, and an objective. By placing the analyzed image between the collimator and the objective, it is possible to observe in the focal plane of the objective a diffraction pattern in which the illumination distribution is proportional to the square of the modulus of the Fourier spectrum of the investigated image. The main methodological shortcoming of this method lies in the impossibility of measuring the phases of the spectrum. It is also inconvenient in practice, since it requires very long exposures for the photography of the diffraction pattern^[14], or else highly sensitive recording photoelectric devices, or finally the use of powerful light sources—lasers. Registration of two-dimensional Fourier spectra is possible also by holographic methods^[15,16], the hologram of the spectrum containing information on the moduli and phases of the harmonic components, but methods of separately extracting this information from the holograms are unknown as yet.

Other methods are based on a direct physical realization of integration by means of formula (1). The gist of these methods reduces to producing, by some optical device, a periodic distribution of illumination on the analyzed photographic image, and then gathering the light flux passing through the image, which is proportional to the product of the distribution of the illumination by the distribution of the transmission coefficient over the image, with the aid of a lens on a photographic receiver (integration). Obviously, in this case a source of incoherent radiation is used.

The first samples of photoelectric spectrum analyzers^[17,19] were intended for the analysis of one-dimensional functions, but even in these instruments the investigated one-dimensional function $f(x)$ was in fact represented by a "two-dimensional" method:

a) either on a photographic plate (film) in such a way that the transmission coefficient T_t at each point along the x axis varied in proportion to the value of the function in identical manner for all values of y , i.e.,

$$T_t(x, y) = T_n(x) = c_1 f(x) \quad \text{for } a < x < b, \quad 0 < y < c$$

(Fig. 1a);

b) or else in the form of a template of the analyzed function, made of opaque material; in this case

$$T_t(x, y) = \begin{cases} 1, & 0 < y < f(x), \\ 0, & y < 0, \quad y > f(x) \end{cases}$$

(Fig. 1b).

The methods of producing a harmonic distribution of the illumination varied. For example, in one of the first spectrum analyzers^[17] they used a long photographic film with a set of images of harmonic functions of multiple frequency, prepared in accordance with the method a). In another instrument^[18] they used a photographic film with an image of a harmonic function, the frequency of which varied smoothly along the film. The coefficient of transmission of the photographic film, with allowance for the dc component, is described by the expression

$$T_h(x, y) = c_2 \cos(px + \theta) + c_3.$$

The light flux gathered by the receiver is proportional to the two-dimensional integral of the product $T_t(x, y)T_h(x, y)$

$$F_\theta(p) = c_4 \int_0^c \int_a^b T_t(x, y) T_h(x, y) dx dy = c_1 c_2 c_4 \int_a^b f(x) \cos(px + \theta) dx + c_5.$$

By measuring $F_\theta(p)$ at values $\theta = 0, \pi/2, \pi, 3\pi/2$, it is possible to exclude the constants and to obtain the sine and cosine components of the Fourier transform of the function $f(x)$. Obviously, the same result is obtained if the image of the function $f(x)$ is prepared by the method b). In this case

$$F_\theta(p) = c_4 \int_0^c \int_a^b T_t(x, y) T_h(x, y) dx dy = c_4 \int_a^b \int_0^{f(x)} T_h(x, y) dx dy = c_4 c_2 \int_a^b f(x) \cos(px + \theta) dx + c_5.$$

A technically better method of producing the harmonic distribution of the illumination is described in^[19,20], where they used an optical system consisting of a glass disc with a harmonic raster, a narrow slit, and a system of spherical and cylindrical lenses. The variation of the period of the distribution of the illumination of the sample was effected by rotating the disc, and the position of the disc relative to the rotation axis was determined by the value of θ . In^[21,22] are described methods of producing harmonic illumination with the aid of periodic rasters superimposed on each other at a certain angle.

As already noted, recently, mainly in connection with the development of methods of statistical analysis

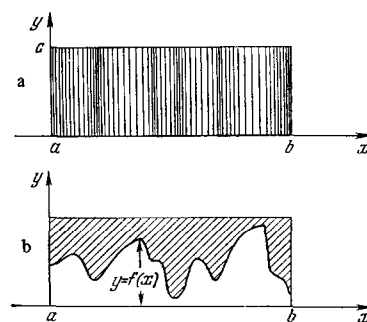


FIG. 1

of random fields, a need arose for apparatus realizing the Fourier analysis of two-dimensional functions.

A two-dimensional function can also be specified in the form of a photographic image made by method a), but in this case the transmission coefficient $T(x, y)$ is a function of two coordinates:

$$T(x, y) = cf(x, y),$$

and its spectrum is accordingly a function of two coordinates (p and q). In "two-dimensional" spectrum analyzers, as in "one-dimensional" ones, a periodic distribution of the illumination is produced on the analyzed sample; different values of the wave numbers p and q are obtained by varying the wavelength of this distribution and by rotating the sample relative to the direction of its spatial orientation. In essence, the principal difference between "two-dimensional" and "one-dimensional" spectrum analyzers lies in the fact that provision is made in the former for rotating the samples. The two-dimensional spectrum analyzers described in the literature, as before, differ in the methods used to produce a periodic distribution of illumination. Thus, besides schemes with harmonic raster illuminators^[23], recently instruments were developed with more perfect although also more complicated illuminators. For example, in some of them, the illuminator is a Michelson interferometer^[24-26]. The constancy of the contrast in the picture of the distribution of the interference fringes when the frequency of the fringes is changed, and the possibility of covering a large frequency band without additional readjustment of the equipment are the main advantages of these devices. These are obtained, however, at a high cost: it is necessary to employ in the instrument quasi-monochromatic light sources, thus inevitably leading to small light fluxes at the output of the interferometer, and as a consequence, to the need of using highly sensitive recording elements; such instruments are quite sensitive to temperature and mechanical vibrations, and are difficult to adjust and to set up.

In^[27,28] are described instruments with a polarization illuminator. It consists of a source of quasimonochromatic light, two Wollaston prisms placed between the analyzer and the polarizer, and two half-wave plates. The prisms are mounted in mounts that are rotated in opposite directions. The periodic picture of dark and light fringes is produced as a result of interference of the components of the ordinary and extraordinary rays, which are separated by a second polarizer (analyzer); the spatial frequency of the fringes changes when the angle of the relative rotation of the optical axis of the Wollaston prisms is changed. As in the preceding case, the light fluxes at the output of the polarization illuminator cannot be very large, and in addition, it is impossible to produce an interference picture of large dimensions with the aid of Wollaston prisms. Such illuminators are most convenient for the analysis of small-structure distributions, for example for the investigation of the spectrum of the graininess of photographic emulsions.

In^[23] is described a setup in which the space-frequency spectrum is measured by scanning the image with a long narrow slit, and by subsequently analyzing the signal from the output of a photocell with an elec-

tronic analyzer. The optical-mechanical parts of such a setup differ little from those of a raster setup, but a more complicated electronic device is necessary to separate the signal.

The foregoing cited articles essentially exhaust the bibliography on two-dimensional spectrum analyzers. In spite of the fact that various spectrum analyzer schemes have been published, the actual apparatus in use, as can be judged from this material, consists apparently of all the isolated samples of instrument models, the constructions of which and the results of measurements performed with them, are little known. In addition, as a rule the articles are devoted to descriptions of instruments intended to solve some one particular problem of interest to the authors; they therefore do not give an idea of the wide possibilities of using two-dimensional spectrum analyzers in a great variety of physical and technical investigations.

The indicated circumstances have stimulated us to present in the present review a detailed description of a two-dimensional spectrum analyzer with a raster illuminator, developed by us, and measurement results illustrating the possible applications of such instruments. Using the raster spectrum analyzers as an example, we can demonstrate most simply and clearly the fundamental principles of optical-electronic methods of realizing two-dimensional Fourier transforms. This is done without cluttering up the exposition by details of the illuminator schemes, which are based at times on rather subtle optical phenomena.

II. OPERATING PRINCIPLE OF A RASTER OPTICAL-ELECTRONIC SPECTRUM ANALYZER

As already noted optical-electronic spectrum analyzers process photographic images of two-dimensional functions of brightness distribution, current distribution, etc. However, this does not limit their capabilities, for under certain conditions it is possible to change over from the image spectra obtained with the aid of the spectrum analyzers to the spectra of the functions themselves. To this end it is necessary first that the linear dimensions in coordinates X and Y differ only in scale (γ) from the dimensions on the image in coordinates x and y respectively, i.e., the following conditions must be satisfied

$$x = \gamma X \text{ and } y = \gamma Y.$$

Further, the connection between the values of the functions $f(X, Y)$ at the point (X, Y) and $f(x, y)$ at the corresponding point (x, y) should be linear, i.e., if $f(x, y)$ is a photograph on a plate, then the transmission coefficient $T(x, y)$ of the photograph and the function $f(X, Y)$ must be connected by the relation

$$T(x, y) = \alpha f(X, Y) + \beta, \quad (8)$$

and β should be small. We shall henceforth put $\beta = 0$. Under these conditions, the spectrum of the initial function

$$f(p, q) = \frac{1}{\alpha \gamma^2} f(p, q), \quad (9)$$

where $f(p, q)$ is the two-dimensional space-frequency spectrum of the image, and p and q are the spatial wave numbers corresponding to the axes x, y , with

$$p = \frac{P}{\gamma} \text{ and } q = \frac{Q}{\gamma},$$

and α is a constant.

Without discussing in the present review methods of linear registration of the function $f(X, Y)$ on photographic plates, we proceed to consider the operating principle of a raster spectrum analyzer.

The simplest construction is that of the spectrum analyzer intended for the measurement of the modulus (or the square of the modulus) of the space-frequency Fourier spectrum of images of definite functions, which interest attaches to the spectrum of the function as a whole, and of its mean value and its variable part. This case includes, in particular, diffraction problems in optics and radio, problems of apodization with the aid of filters that introduce no phase shifts, etc.

Let us consider the action of the optical spectrum-analyzer scheme shown in Fig. 2.* Light from the source 1, with the aid of an illuminator consisting of condenser 2 and a narrow long slit 3, passes through a raster 4 having a periodic transparency distribution, and falls, in the form of a system of alternating light and dark fringes, on the analyzed object 5. The object is mounted on a frame rotating around the optical axis. The light flux passing through the object is gathered by a condenser 6 on a photocell 7. The condenser is placed in such a position, that the image of the slit of the illuminator is projected on the cathode of the photocell: in this case, the image will not shift over the photocathode regardless of the position of the sample or of the raster. To decrease the influence of aberrations of the condenser and of the inhomogeneity of the distribution of the sensitivity over the photocathode on the measurement result, sometimes an intermediate diaphragm and an additional condenser are used, as shown in Fig. 2.

Let us find an expression for the flux directed by the condenser on the photocell. To this end we introduce in the object plane two systems of coordinates, a fixed one $\xi O \eta$, connected with the fixed base of the instrument, and a moving one xOy , which is connected with the frame in which the object is mounted. The moving system of coordinates can rotate (together with the frame) relative to the stationary system around a common center which coincides with the optical axis (Fig. 3).

The raster made in the form of a periodic grating consisting of a system of transparent and opaque strips that lie parallel to the illuminator slit, can be moved along the optical axis between the slit and the

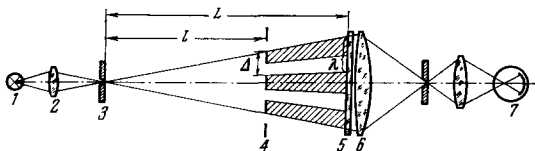


FIG. 2

*This scheme was developed by N. S. Shestov in 1961 and independently by Uberoi [23] in the U.S.A., who published a similar scheme in 1962.

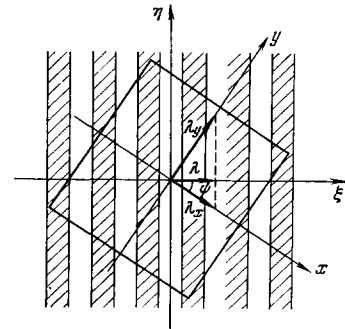


FIG. 3

frame. Depending on the pitch of the raster Δ (Fig. 2) and its position, which is determined by the distance from the slit to the raster l and to the object L , a system of dark and light fringes of definite width is produced on the object. The law governing the distribution of the illumination in this periodic system of fringes is a complicated function, the form of which depends not only on the indicated geometrical factors but also on the influence of the half-shadows (owing to the finite width of the slits), the diffraction of light by the element of the raster, errors in preparing the raster, etc. We represent this function by a Fourier series in the stationary coordinate system, recognizing that the raster lines are parallel to the y axis:

$$E(\xi, \eta) = E_0 + E_1 \cos(k\xi) + \dots + E_i \cos(ik\xi) + \dots \quad (10)$$

Here $k = 2\pi/\lambda$ is the spatial wave number, E_0 is the average value of the illumination, and E_i is the amplitude of the i -th harmonic.

We now introduce the motion of the raster in a direction perpendicular to the optical axis (and to the strips of the raster) with a constant velocity v_r . We then obtain for the illumination distribution moving over the object the expression

$$E(\xi, \eta, t) = E_0 + E_1 \cos(k\xi + \omega t) + E_2 \cos 2(k\xi + \omega t) + \dots, \quad (11)$$

where ω is the cyclic temporal frequency.

To obtain two-dimensional space-frequency spectra, provision is made for rotating the object (with the aid of the rotating frame) relative to the direction of the illuminating fringes. The moving system of coordinates rotates together with the object. The coordinates x and y of the moving system and ξ of the stationary system are connected by the transformation

$$\xi = x \cos \psi + y \sin \psi,$$

where ψ is the angle of rotation of the moving axis relative to the stationary one (see Fig. 3).

The distribution of the illumination in the moving axis is

$$E(x, y, t) = E_0 + E_1 \cos(px + qy + \omega t) + \dots, \quad (12)$$

where

$$k \cos \psi = p, \quad k \sin \psi = q.$$

Substituting the value of k and introducing the notation

$$\frac{\lambda}{\cos \psi} = \lambda_x \text{ and } \frac{\lambda}{\sin \psi} = \lambda_y,$$

we obtain

$$p = \frac{2\pi}{\lambda_x} \text{ and } q = \frac{2\pi}{\lambda_y}.$$

It follows from Fig. 3 that λ_x and λ_y are the projections of the wavelength λ of the illumination distribution on the axes x and y , and consequently p and q have the meaning of spatial wave numbers corresponding to the axes x and y .

The (integrated) light flux gathered by the condenser is proportional to the product of the distribution of the illumination $E(x, y, t)$ by the distribution of the transmission coefficient $T(x, y)$ over the object:

$$F(p, q, t) = \iint_{(S)} E(x, y, t) T(x, y) dx dy$$

$$= E_0 \iint_{(S)} T(x, y) dx dy + E_1 \iint_{(S)} T(x, y) \cos(px + qy + \omega t) dx dy + \dots \quad (13)$$

where S is the area of the analyzed sample. The first term of the series is the mean value of the flux. In the integrand of the second term, we expand the cosine of the sum into components, and obtain

$$F_1(p, q, t) = E_1 \left[\cos \omega t \iint_{(S)} T(x, y) \cos(px + qy) dx dy - \sin \omega t \iint_{(S)} T(x, y) \sin(px + qy) dx dy \right] \quad (14)$$

Taking into account the notation used in (2)–(6), expression (14) takes the form

$$F_1(p, q, t) = E_1 [J_{\cos}(p, q) \cos \omega t - J_{\sin}(p, q) \sin \omega t]$$

$$= E_1 |f(p, q)| \cos[\omega t - \varphi(p, q)] \quad (15)$$

Here $|f(p, q)|$ is the sought modulus of the space-time Fourier spectrum, and $\varphi(p, q)$ is the phase of the spectrum.

The signal at the output of the photocell with sensitivity ϵ is

$$U = \epsilon F(p, q, t).$$

It contains the dc component and the ac components with frequencies $\omega, 2\omega, 3\omega, \dots$. We note that the amplitude of the second harmonic of the signal is proportional to the modulus of the Fourier spectrum for the second spatial harmonic of the illumination distribution, the amplitude of the third harmonic of the signal is proportional to the modulus of the spectrum for the third spatial harmonic, etc. If a narrow-band amplifier tuned to a frequency $f = \omega/2\pi$, with a gain K , is placed behind the photocell, then the signal at the output of such an amplifier will be

$$U_1(t) = K\epsilon F_1(p, q, t) = K\epsilon E_1 |f(p, q)| \cos(\omega t - \varphi) \quad (16)$$

since the dc component and all the harmonics except the first will not be passed by the filter.

Thus, when the raster moves, the signal at the output of the tuned amplifier varies harmonically, and the amplitude of the oscillations is proportional to the modulus of the Fourier spectrum of the investigated object, which is secured in the frame.

It is easy to demonstrate a very important property of the raster system, namely that the frequency of the first harmonic of the signal at the output of the receiver does not depend on the position of the raster. If λ is the wavelength of the distribution of the illumination in the plane of the object, and T is the period of the oscillation of the illumination at the given points of the image in time, then by regarding the rate of displacement v of the illumination picture over the

sample as the rate of displacement of a constant-phase line, we obtain

$$|v| = \frac{\lambda}{T}.$$

From Fig. 2 we get

$$\lambda = \Delta \frac{L}{l} \text{ and } v = v_r \frac{L}{l},$$

hence

$$T = \frac{\Delta}{|v_r|} \quad \text{и} \quad \omega = \frac{2\pi}{T} = 2\pi \frac{|v_r|}{\Delta}.$$

If the velocity v_r of the raster is constant, we have $\omega = \text{const}$. Because of this property of the raster scheme, we can use the advantages of narrow-band amplification of the alternating current. What is particularly important, it is possible to use rasters with any periodic (not necessarily harmonic) transparency distribution.

In the general case the two-dimensional spectrum is the surface of complicated form. An idea of the form of this surface, depending on the complexity, can be obtained using a larger or smaller number of values of the spectrum at discrete points (discrete values of p and q) or from a set of radial (the angle of rotation ψ is fixed, and the raster moves along the optical axis), or circular (the position of the raster is fixed and the object is rotated about the optical axis) sections of the spectrum (Fig. 4). We note that it suffices to rotate the object in the interval from zero to 180° , since the two-dimensional Fourier spectrum is symmetrical with respect to the origin:

$$f(p, q) = f^*(-p, -q) \text{ and } f(p, -q) = f^*(-p, q),$$

from which

$$|f(p, q)| = |f(-p, -q)|, \quad |f(p, -q)| = |f(-p, q)|$$

and

$$\varphi(p, q) = -\varphi(-p, -q), \quad \varphi(p, -q) = -\varphi(-p, q).$$

To carry out absolute measurements, the instrument is calibrated beforehand against objects with known spectra.

The main factor limiting the technical capabilities of the raster spectrum analyzer is the variation of the contrast in the illumination distribution, due to the diffraction of the light by the elements of the raster, and consequently to the variation of the amplitude of the first harmonic of the signal, as a function of the position of the raster on the optical axis. The influence of diffraction can be estimated by using the expressions for the ratio of the half-width of the central dif-

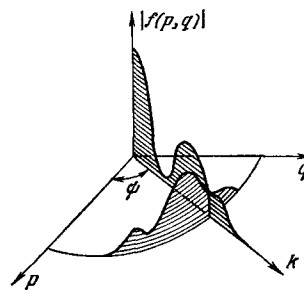


FIG. 4

fraction maximum r_d of a transparent strip to the wavelength λ ;

$$\frac{r_d}{\lambda} = 2 \frac{(L-l)l}{L} \frac{\lambda l}{\Delta^2}.$$

By specifying the permissible relative broadening (r_d/λ) and the pitch Δ of the raster, we determine the maximum dimension L , and consequently the region of the spatial frequencies that can be covered by a given instrument. Obviously, to decrease the influence of diffraction it is best to use a light source with an intense shortwave radiation λ_l and rasters with a large pitch. In measurements of very high precision it is possible, by analyzing an object with a known spectrum, to determine for all values of l the correction coefficients and to take them into account in the reduction of the recorded spectra. It should be noted that interference methods of producing a periodic illumination distribution are free of this limitation.

III. DESCRIPTION OF SPECTRUM ANALYZER. INVESTIGATION OF THE SPACE-FREQUENCY SPECTRA OF DEFINITE FUNCTIONS

The described operating principle is the basis for the raster spectrum analyzer constructed by us. An overall view of the instruments is shown in Fig. 5. The construction of the instrument made it possible to analyze images obtained on photographic plates and films measuring 60×60 mm. The objects were mounted in a frame, which could be rotated about the optical axis in a range of 118° . A glass raster with a rectangular grid of lines with a period $\Delta = 0.4$ mm was moved smoothly along the optical axis between the slits of the illuminator (width of slit 0.05 mm) and the frame in a range from 10 to 180 mm, corresponding to the range of variation of the spatial wavelength λ from 0.6 to 11.2 mm or wave numbers k from 10.8 to 0.56 rad/mm.

The motion of the raster in a direction perpendicular to the optical axis was with the aid of a cam with a profile in the form of a bilateral Archimedes spiral. Such a cam ensures a constant velocity of motion of the raster with small loss of time for reversing the direction of motion. The raster velocity v_r was ~ 100 mm/sec.

The spectra were registered on paper charts of an automatic recorder specially built into the instrument. Rotation of the automatic recorded drum could be performed, at will, either in synchronism with the rota-

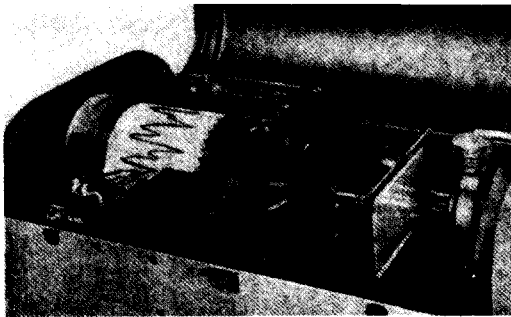


FIG. 5

tion of the frame (circular sections) or with the displacement of the raster along the optical axis (radial sections). In the former case the spectrum was registered as a function of the rotation angle ψ with a scale 0.85 mm/deg, and in the latter case the spectrum was a function of the wave number k (rad/mm). The scale of the recording was 31.9 mm/(rad/mm).

The use of linear and quadratic detectors, and also of a logarithmic amplifier, made it possible to register the moduli of the spectra in linear, quadratic, and logarithmic scales. The relative error of the measurements in this model was 1–2%.

To illustrate the operation of the spectrum analyzer let us consider plots of spectra of very simple definite functions, representing diaphragms (pupils) of various shapes with constant value of transmission $T(x, y)$ within the limits of the diaphragm aperture.

Returning to formula (14), we get an expression for the spectrum of such definite functions, bearing in mind the constancy of $T(T(x, y) = \bar{T} = \text{const})$:

$$F_1(p, q, t) = E_1 \bar{T} \left[\cos \omega t \int_{(S)} \cos(px + qy) dx dy - \sin \omega t \int_{(S)} \sin(px + qy) dx dy \right] = E_1 |f(p, q)| \cos(\omega t - \varphi),$$

i.e., the form of the spectrum $|f(p, q)|$ will be determined in this case only by the form of the contour bounding the area S over which the integration is carried out. If S is symmetrical with respect to the axes x and y , then, recognizing that integrals of odd functions between symmetrical limits vanish, we get

$$f(p, q) = \bar{T} \int_{(S)} \cos(px + qy) dx dy. \quad (17)$$

The solution of this equation, for example in the case when the contour is a circle of diameter D_1 , yields

$$|f(k)|^2 = S \left[\frac{2J_1(z_1)}{z_1} \right]^2, \quad (18)$$

where S is the area of the circle, $J_1(z_1)$ is a Bessel function of the first kind,

$$z_1 = k \frac{D_1}{2} = \frac{2\pi}{\lambda} \frac{D_1}{2},$$

and k is the spatial wave number. It is known at the same time that the illumination $E(\psi)$ produced in the focal plane of the objective by a beam of rays diffracted at an angle ψ , on a circular aperture of diameter D_2 , is given by the expression

$$E(\psi) = E_0 \left[\frac{2J_1(z_2)}{z_2} \right]^2, \quad (18')$$

where E_0 is the illumination at the center of the diffraction pattern

$$z_2 = k l \frac{D_2}{2} \sin \psi \cong \frac{2\pi}{\lambda l} \frac{D_2}{2} \frac{r}{F},$$

λ_l is the wavelength of the light, r is the distance from the central maximum, and F is the focal distance of the objective. From a comparison of (18') with (18) we see that $|f(k)|^2$ describes, accurate to a constant factor, the distribution of the illumination in the diffraction pattern observed from an aperture of round form.

Equating z_1 and z_2 , we can find the scale factor γ :

$$k \frac{D_1}{2} = k_1 \frac{D_2}{2} \frac{r}{F},$$

whence

$$\gamma = \frac{k_1}{k} = \frac{D_2}{D_1} \frac{r}{F}. \quad (19)$$

It can be shown^[4] that a similar relation exists between the arguments of functions describing the spectra and the form of the diffraction pattern also for pupils of all other shapes. Thus, plots of spectra of pupil images make it possible to determine uniquely the form of the diffraction pattern from such pupils.

Figure 6 shows plots of the radial sections of the spectra of one and two rectangular pupils (slits) of different dimensions. The plots are logarithmic. The logarithm of the modulus of the spectrum of two slits of equal width $2r_0$, located at a distance $2d$, is conveniently represented in the form

$$\lg |f(k)| = \lg c + \lg \left(\frac{1}{|k|} \right) + \lg |\sin kx_0| + \lg \left| \sin \left(kd + \frac{\pi}{2} \right) \right|. \quad (20)$$

The constant c depends here on the dimension of the slits and on the gain of the amplifier. For convenience in comparison, spectra on the same plots were recorded at equal values of c .

In expression (19), the term $\log(1/|k|)$ does not depend on the dimension and on the number of the slits, and always serves as the envelope of the spectra. In the plots, the envelope (dashed line) is constructed from the calculated data.

Adding to the envelope the next term, we obtain the form of the spectrum of one slit (curves 1), and then, taking the last term into account, we obtain the spectrum of two slits (curves 2). The second diagram from

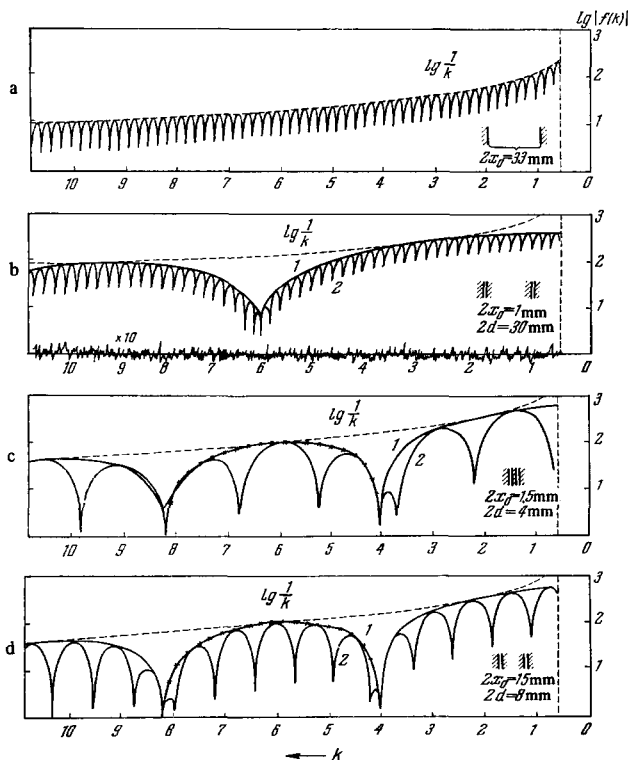


FIG. 6

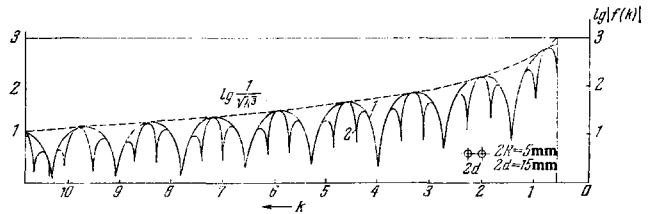


FIG. 7

the top shows in addition the noise of the apparatus with the gain increased by a factor of 10.

Similar spectra of one round aperture (curve 1) and two such apertures (curve 2) are shown in Fig. 7. In this case the plot of the envelope is given by $\log(1/\sqrt{|k|^3})$.

In the first variant of the spectrum analyzer, the structural features determined the minimum value of $k = 0.56$ rad/mm ($\lambda = 11.2$ mm) at a raster pitch $\Delta = 0.4$ mm, as a result of which, at large diaphragm dimensions, a part of the spectrum near the central maximum may not be registered, but on the other hand, the high orders of the spectrum will be well represented (see, for example, Fig. 6a). By analyzing diaphragms of the same shape but of smaller width, it is possible to record in greater detail the region of the spectrum near the central maximum (Fig. 6b, curve 1); in principle, the origin of the plot can be conveniently close to the center of the diffraction pattern.

Figure 8 illustrates the form of circular sections (for two values of k) of the spectra of a radial target pattern consisting of 36 pairs of transparent and opaque sectors.

Figure 9 shows a section of a two-dimensional spectrum of a diaphragm consisting of regularly arranged circular apertures. For the sake of clarity, the plots were recorded with shifted zero levels. Naturally, the form of the apertures and their location are of no importance at all for the analysis process.

The presented illustrative material apparently demonstrates quite convincingly the great possibilities of optical-electronic spectrum analyzers with respect to the study of diffraction phenomena. With the aid of these instruments it is possible to investigate just as easily diffraction pictures from either one aperture of an arbitrary shape and arbitrary dimension, or from an aggregate of apertures of different shapes and dimensions, arbitrarily oriented on a plane.

The spectrum analyzer is very convenient for the investigation and choice of apodizing diaphragms. In^[20] is calculated the shape of a diaphragm intended to increase the resolving power of objectives by redistribut-

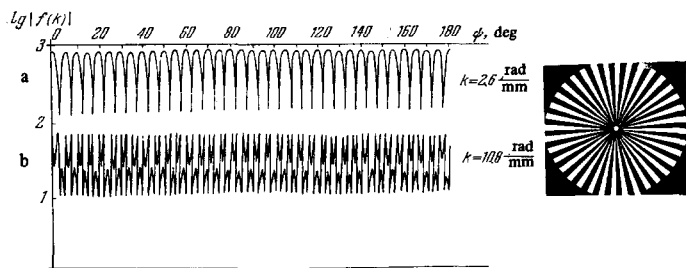


FIG. 8

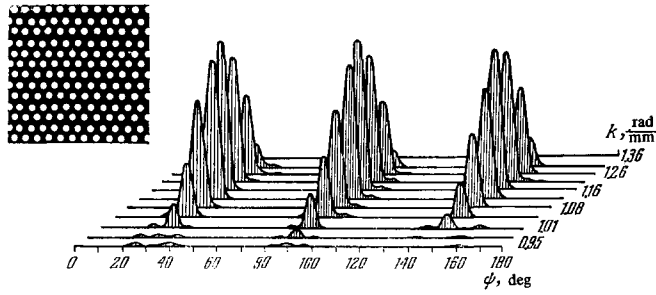


FIG. 9

ing the energy in the diffraction orders, at which the first lateral maximum should vanish. We have prepared such a diaphragm and plotted its spectrum (Fig. 10, curve 1). For comparison, the same figure shows the spectrum of the diaphragm in the form of a square of equal area (curve 2). The curves agree well with those calculated in^[29]; the presence of a weak maximum in a first order is due to the insufficiently accurate construction of the diaphragm.

Taking the inverse Fourier transform, i.e., finding the form of the function from the specified spectrum (representing a curve determining the desirable form of the spectrum), it is possible to determine the form of the corresponding apodizing diaphragm. In order to illustrate the possibility of using the instrument to solve similar problems, we have obtained the direct and inverse Fourier transforms of a very simple function in the form of a triangle.

To this end, we first recorded the spectrum of a diaphragm in the form of an isosceles triangle (direct transform). We recall that the spectrum of the triangle is described by the function

$$f(k) = c \left(\frac{\sin z}{z} \right)^2.$$

We prepared a diaphragm (Fig. 11) corresponding to this plot, with a contour consisting of a central lobe and two side lobes of the spectrum of the triangle. We then plotted the spectrum of this diaphragm, i.e., the inverse transform, yielding the initial function. The obtained spectrum is shown by the solid line in Fig. 11. The curve corresponds sufficiently well to one branch of the triangle; the smooth transitions to the zero line and to the axis of the triangle are due to the fact that in the construction of the diaphragm no account was taken of the higher-order maxima in the spectrum.

The dashed line of Fig. 11 shows the form of the function whose spectrum has only one central maximum without secondary diffraction maxima. This function is a result of the transformation of the same diaphragm,

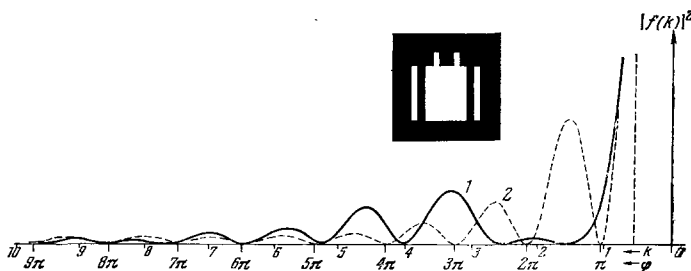


FIG. 10

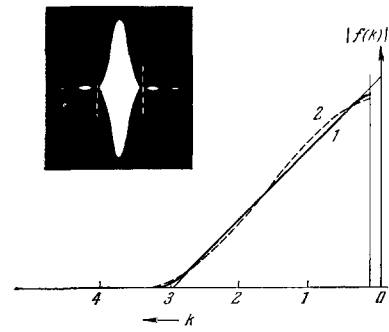


FIG. 11

but with the side lobes covered. It should be noted that the curves of Fig. 11 were obtained after introducing certain improvements in the instrument, which made it possible to start the plotting with $k = 0.14$.

It is perfectly obvious that the spectrum analyzer can be used for the investigation of more complicated cases of apodization, in which not only the form of the diaphragm is chosen, but also the transmission coefficient over the aperture of each frame is varied, i.e., amplitude filters are used, or else both simultaneously.

The possibility of obtaining the inverse Fourier transforms of functions of arbitrary specified form is highly promising for the choice of apodizing filters. However, the simplest spectrum analyzer makes it possible to solve this problem only for the case when the analyzed functions have no negative values. This difficulty can be circumvented in principle by introducing into the instrument a device making it possible to separate the spectra of the positive and negative parts of the investigated functions. One such method is to use "two-color" images of the function. In this case, the parts of the diaphragm corresponding to the positive and negative functions should transmit beams of light of different spectral composition. These beams are separated beyond the condenser and are directed to two photoreceivers. The beams can be separated with the aid of a splitting plate or a biprism with two appropriate optical filters. The difference between the signals of the photoreceivers proportional to the difference of the spectra of the positive and negative parts of the investigated function is registered by the automatic plotter of the instrument.

For many problems it suffices to know the modulus of the Fourier spectrum, but cases are possible, when it is necessary to measure also the phases of the spectrum. The method measuring the phase $\varphi(p, q)$ follows from formula (16): it is necessary to form in the instrument a signal with phase ωt and determine the phase difference of the signals

$$|(\omega t - \varphi) - \omega t| = \varphi.$$

To this end it is possible, for example, to mount a narrow slit over the frame window in the object plane, directly over the optical axis; the long side of the slit should be parallel to the lines of the raster. The light flux passing through the raster and the slit is gathered by condenser on a separate photoreceiver. Recognizing that in the stationary coordinate the slit is symmetrical with respect to the line $\xi = 0$, we obtain an expression for the flux passing through the slit:

$$F_{sl}(0, \eta, t) = E(0, \eta, t) S_{sl} = E_0 S_{sl} + E_1 S_{sl} \cos \omega t + \dots, \quad (21)$$

where S_{sl} is the area of the slit.

By placing behind the photoreceiver an amplifier tuned to the frequency $f = \omega/2\pi$, we obtain at the amplifier output a signal with phase ωt at any position of the raster on the optical axis. The phase difference of the signals from the outputs of the resonant amplifiers of the channels with the object and with the slit can be measured with the aid of an ordinary electronic phase meter whose output signal is independent of the input-signal amplitudes, but is proportional to the phase difference of these signals. In formulas (16) and (21) it is also necessary to take into account the initial phases, which are determined by the position of the image of the raster relative to the center of the object and the central line of the slit at the instant of the start of motion of the raster. However, if the slit is sufficiently narrow and is installed directly over the center of the object, which coincides with the optical axis, the initial phases will be equal and will cancel out upon subtraction in the phase meter. It is possible to check the equality of the phases by using the signal from the slit and the signal from a control object in the form of a similar slit, located at the center of the frame.

To obtain a reference signal with phase ωt , it is possible to use also a separate photoelectric channel with its own light source and receiver. The optical axis of this channel should be strictly parallel to the optical axis of the channel with the object. The raster for both channels should be common. The distance between the optical axis of the channels should be equal to an integer number of raster periods—in this case no initial phase difference of the signals is produced. Examples of plots of the phase of the Fourier spectrum simultaneously with the modulus of the spectrum are shown in Figs. 12 and 13. Figure 12 shows the spectrum of a rectangular aperture 16 mm wide, located almost symmetrically relative to the optical axis of the measuring channel (the shift does not exceed 0.1

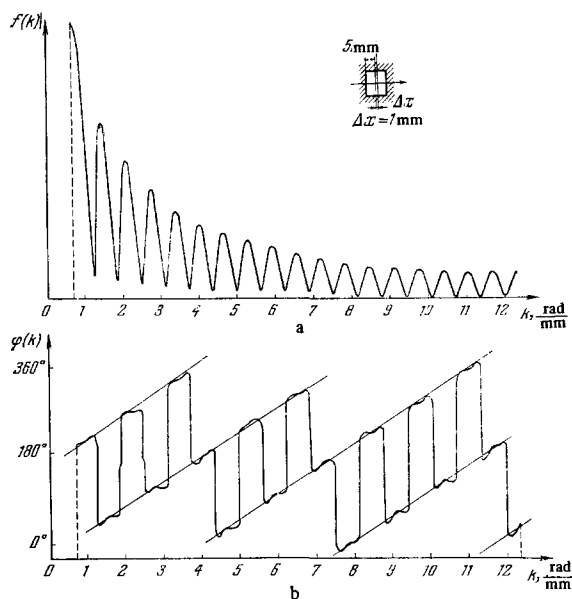


FIG. 13

mm). On the upper curve is shown a section of the modulus of the spectrum, having the form $|\sin z/z|$, and the lower one shows a section of the phase, which for this function assumes alternately the values 0° and 180° on intervals lying between the zeroes of the modulus. Figure 13 shows the spectrum of a rectangular aperture 10 mm wide, shifted relative to the optical axis by 0.9 mm. In this case, in accordance with the shift theorem, the phase of the spectrum will contain a term that increases linearly with the frequency. The proportionality coefficient is equal to the value of the shift, which is well confirmed by the presented plot.

IV. INVESTIGATION OF THE SPACE-FREQUENCY ENERGY SPECTRA OF IMAGES OF RANDOM TWO-DIMENSIONAL FUNCTIONS

So far we have discussed the question of measuring spectra of definite two-dimensional functions. Let us consider now the possibility of using a spectrum analyzer to investigate spectra of images of random two-dimensional functions, describing, for example, the distribution of the brightness over the surface of the sun, the earth, a cloud layer, or a water surface, the distribution of the transmission coefficient over the plane of uniformly exposed photographic material, or the coefficient of reflection from a matte surface, the distribution of the transmission coefficient of the turbulent layer of liquid or gas, etc.

One of the most widely used characteristics of random functions is the space-frequency energy spectrum or power spectrum. Usually, in technical applications, interest attaches to the power spectrum of the fluctuations of random processes, i.e., to the energy spectrum of local random oscillations of the values of the function relative to the average level, averaged over the area, namely the dc component of the process.

Let a section of area S_0 of a random field, which will be assumed to be stationary and ergodic, be described by the function

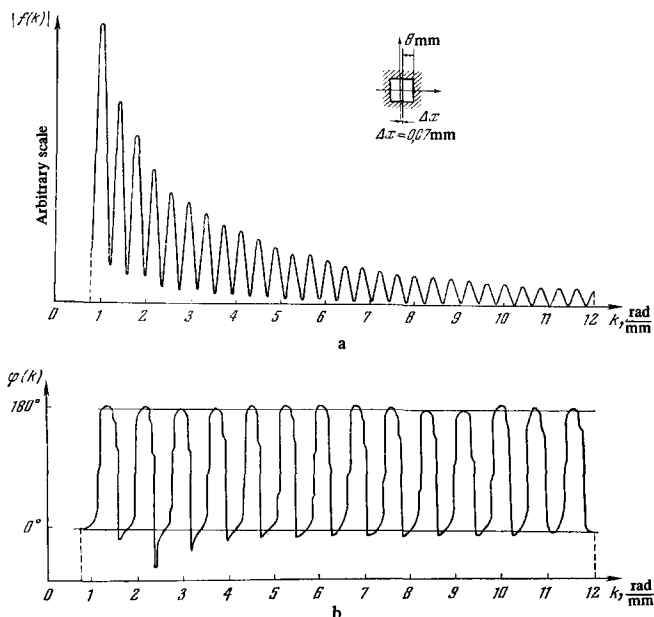


FIG. 12

$$f_{S_0}^e(X, Y) = (\bar{f}_{S_0}) + f_{S_0}(X, Y); \tag{22}$$

Here \bar{f}_{S_0} is the dc component and $f_{S_0}(S, Y)$ is the fluctuating component. Then the spectrum of the power of the fluctuations of the random field is determined by the relations

$$G(P, Q) = \lim_{S_0 \rightarrow \infty} \frac{|f_{S_0}(P, Q)|^2}{S_0}. \tag{23}$$

In practice, one analyzes the realizations of sections of the field having finite dimensions S_0 . Averaging a large number ($N \gg 1$) of spectra from different sections of the field yields an estimate of the power spectrum of the entire field, in the form

$$\frac{1}{NS_0} \sum_{i=1}^N |f_{S_{0i}}(P, Q)|^2. \tag{24}$$

The transmission function of the analyzed photographs of the section of the random field will, in accordance with (22), be of the form

$$T_0(x, y) = \bar{T} + T(x, y).$$

In this case we obtain in lieu of (14) the following expression for the flux gathered by the condenser on the photoreceiver:

$$F_1(p, q, t) = E_1 \bar{T} \iint_{(S_0)} \cos(px + qy + \omega t) dx dy + E_1 \iint_{(S_0)} T(x, y) \cos(px + qy + \omega t) dx dy.$$

If the frame has a symmetrical form, we have

$$F_1(p, q, t) = E_1 \bar{T} \cos \omega t \iint_{(S_0)} \cos(px + qy) dx dy + E_1 \cos[\omega t - \varphi_{S_0}(p, q)] |f_{S_0}(p, q)| = F_t + F_m, \tag{25}$$

where $|f_{S_0}(p, q)|$ and $\varphi_{S_0}(p, q)$ are the modulus and argument (phase) of the spectrum of the transparency fluctuations.

It follows from (23) and (24) that as a result of the measurements it is necessary to obtain an undistorted value of the quantity $|f_{S_0}(p, q)|$. The first term F_t in (25) describes the spectrum of the dc components, and its form, as we already know (see (17)) is determined by the form of the frame. In this case it will distort the measured fluctuation spectrum. To decrease this distortion, it is possible to use apodizing filters either in the form of diaphragms of different shapes, or amplitude filters, which in this case are of great interest, since their application does not lead to a decrease of the investigated area of the realization. Let us consider the action of an apodizing amplitude filter for the case when the frame is a rectangle with area $S_0 = 2x_0 2y_0$. Without the filter, F_t for a rectangle is given by

$$F_t = E_1 \bar{T} S_0 \frac{\sin px_0}{px_0} \frac{\sin qy_0}{qy_0} \cos \omega t. \tag{26}$$

At high frequencies, a function of the type $\sin z/z$ tends to zero, and consequently the distortions due to F_t will be small. At low frequencies, the distortions can be quite large, particularly if account is taken of the fact that the amplitudes of the individual harmonics of the spectrum are always small compared with \bar{T} .

By placing over the object a filter with a specified

transmission function $T_f(x, y)$, we get in lieu of F_t

$$F_{t..f} = E_1 \bar{T} \cos \omega t \iint_{(S_0)} T_f(x, y) \cos(px + qy) dx dy. \tag{27}$$

By choosing $T_f(x, y)$ we can obtain upon integration a function that decreases with increasing frequency much more rapidly than $(\sin px_0/px_0) (\sin qy_0/qy_0)$. It is obvious that $T_f(x, y)$ should have a maximum at the center at $x = 0$ and $y = 0$, and should drop off monotonically towards the edges of the frame. Under these conditions, the filter influences most strongly the value of the dc components, and has less of an effect on the "semantic" content of the image, characterized by $T(x, y)$.

Let us use a filter with a transmission function in the simple form

$$T_f(x, y) = \cos \frac{\pi x}{2x_0} \cdot \cos \frac{\pi y}{2y_0}. \tag{28}$$

For this filter we obtain

$$F_{t..f} = E_1 \bar{T} S_0 \cos \omega t \cdot \frac{(-1) \cos px_0 (-1) \cos qy_0}{(2px_0)^2 - \pi^2 (2qy_0)^2 - \pi^2}. \tag{29}$$

Figure 14 shows the transmission functions of the frame window with and without filters, and Fig. 15 shows their calculated spectra (in relative units) for the particular case when $q = 0$, i.e., for spatial harmonics whose wave crests are parallel to the y axis. It is clearly seen that when the filter is used, the relative magnitude of the side maxima compared with the fundamental maxima decreases; for example, at the frequency p' marked on Fig. 15, the amplitude of the side maxima is decreased by a factor of 10 by a filter of the type (28). The best results can be obtained with filters having a nearly-bell-shaped transmission function. For example, at the same frequency, the magnitude of the side maxima for filters with

$$T_f(x, y) = \cos^3 \frac{\pi x}{2x_0} \cdot \cos^3 \frac{\pi y}{2y_0} \tag{30}$$

decreases by approximately 200 times (see Fig. 15).

Different types of apodizing filters are considered in articles devoted to apodization^[4,30].

It should be noted that the use of filters decreases not only the magnitude of the side maxima compared with the fundamental maximum, but also the absolute value of the fundamental maximum. Thus, for the filter (28), the amplitudes of all the harmonics of the spectrum decrease to a value 0.405, and for the filter (30) they decrease to 0.18 of the value obtained when the analysis is carried out without a filter. This makes it necessary to use more powerful light sources in the illuminators, and amplifiers with large gain.

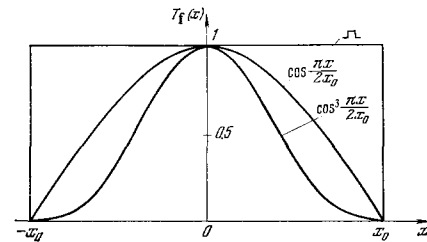


FIG. 14

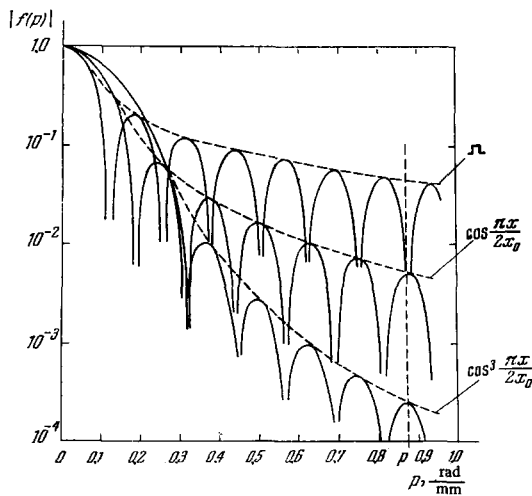


FIG. 15

Let us consider now the influence of the filter on the measured spectrum of the fluctuations. When the filter is used, we get in lieu of FM

$$F_{m,f}(p, q, t) = E_1 \iint_{(S_0)} T(x, y) T_0(x, y) \cos(px + qy + \omega t) dx dy, \quad (31)$$

which yields, for example for the filter (28),

$$\begin{aligned} F_{m,f}(p, q, t) = & E_1 \cos \omega t \cdot \frac{1}{4} \left\{ \iint_{(S_0)} T(x, y) \cos \left[\left(p + \frac{\pi}{2x_0} \right) x + \left(q + \frac{\pi}{2y_0} \right) y \right] dx dy \right. \\ & + \iint_{(S_0)} T(x, y) \cos \left[\left(p + \frac{\pi}{2x_0} \right) x + \left(q - \frac{\pi}{2y_0} \right) y \right] dx dy \\ & + \iint_{(S_0)} T(x, y) \cos \left[\left(p - \frac{\pi}{2x_0} \right) x + \left(q + \frac{\pi}{2y_0} \right) y \right] dx dy \\ & \left. + \iint_{(S_0)} T(x, y) \cos \left[\left(p - \frac{\pi}{2x_0} \right) x + \left(q - \frac{\pi}{2y_0} \right) y \right] dx dy \right\} \\ & - E_1 \sin \omega t \cdot \frac{1}{4} \left\{ \iint_{(S_0)} T(x, y) \sin \left[\left(p + \frac{\pi}{2x_0} \right) x + \left(q + \frac{\pi}{2y_0} \right) y \right] dx dy \right. \\ & + \iint_{(S_0)} T(x, y) \sin \left[\left(p + \frac{\pi}{2x_0} \right) x + \left(q - \frac{\pi}{2y_0} \right) y \right] dx dy \\ & + \iint_{(S_0)} T(x, y) \sin \left[\left(p - \frac{\pi}{2x_0} \right) x + \left(q + \frac{\pi}{2y_0} \right) y \right] dx dy \\ & \left. + \iint_{(S_0)} T(x, y) \sin \left[\left(p - \frac{\pi}{2x_0} \right) x + \left(q - \frac{\pi}{2y_0} \right) y \right] dx dy \right\}. \end{aligned} \quad (32)$$

We put

$$\frac{1}{4} \{ J_1 \cos + J_2 \cos + J_3 \cos + J_4 \cos \} = \bar{J}_{\cos},$$

$$\frac{1}{4} \{ J_1 \sin + J_2 \sin + J_3 \sin + J_4 \sin \} = \bar{J}_{\sin};$$

Then (31) can be represented in the form

$$F_{m,f}(p, q, t) = E_1 |\bar{f}_{S_0}(p, q)| \cos[\omega t - \varphi_{S_0}(p, q)]. \quad (33)$$

It follows from (32) and (33) that when the filter (28) is used the value of the fluctuation spectrum of the wave numbers (p, q) is the arithmetic mean of the values of the spectrum for $(p \pm \pi/2x_0, q \pm \pi/2y_0)$, and that the instrument registers at its output already the result of the averaging. The action of filters with a transmission function different from (28) is similar, but the number and position of the wave numbers in the vicinity of (p, q) , for which the values of the spec-

tra are averaged, and the weight factor with which the value of the spectrum at the given point enters in the total result, will vary in accordance with the type of $T_f(x, y)$.

We note that the averaging effected by the instrument is equivalent to the smoothing of the spectrum of a given object or, in other words, to measurement of the spectrum with a worse resolution.

The use of the filter thus leads to a certain deterioration of the resolution of the analyzer, but this effect produces even favorable results in the analysis of random functions, for this increases the averaging of the random oscillations in the spectrum of one image, and consequently it is necessary to have a smaller number of spectra of different images to obtain statistical estimates. The resolving power of two-dimensional spectrum analyzers is characterized by a figure on the pOq plane. The dimensions and shape of the figure are determined by the chosen resolution criterion, by the dimensions and form of the frame, and in the presence of an apodizing filter also by the law governing the distribution of the transparency over the filter. Any cross section of this figure, passing through its symmetry center, is a linear resolution in a given direction, determined in the same manner as for the one-dimensional case. The question of a rigorous definition of a resolution criterion for the two-dimensional case is not perfectly clear at present.

¹ P. M. Duffieux, *L'intégrale de Fourier et ses applications à l'optique*, Université de Besançon.

² P. Elias, D. S. Gray, and D. Z. Robinson, *JOSA* 42, (2), 127 (1952).

³ A. Marechal and M. Francon, *The Structure of the Optical Image* (Russian translation), Mir, 1964.

⁴ P. Jaquinot and B. Roisen-Dossier, *Progress in Optics, Apodisation*, vol. 3, Amsterdam, 1964.

⁵ E. G. Zelkin, *Postroenie izluchayushchei sistemy po zadanoi diagramme napravlenosti* (Construction of a Radiating System from a Specified Directivity Pattern), Gosenergoizdat, 1963.

⁶ M. S. Sheskov, *Vydelenie opticheskikh signalov na fone sluchainykh pomekh* (Separation of Optical Signals Against the Background of Random Noise), Soviet Radio, 1967.

⁷ J. A. Jamieson, R. H. McFee et al., *Infrared Physics and Engineering*, McGraw-Hill, 1963.

⁸ Z. P. Horwitz and G. L. Shelton, *Proc. IRE* 49 (1), 175 (1961).

⁹ P. Mertz and F. Gray, *BST Journ.* 13 (3), 464 (1934).

¹⁰ E. L. Orlovskii and A. M. Khalfin, et al. *Teoreticheskie osnovy élektricheskoi peredachi izobrazhenii* (Theoretical Fundamentals of Electric Image Transmission), Soviet Radio, 1962.

¹¹ In: *Principles of Electronic Television* (F. Schroter, ed.), Energiya, 1965.

¹² F. Perrin, *Jour. SMPTE* 69, 151 and 239 (1960).

¹³ L. J. Cutrona et al., *Trans. Inst. Radio Engrs. JT-6*, 386 (1960).

¹⁴ F. S. Harris, *Applied Optics*, 3 (8), 909 (1964).

¹⁵ G. W. Stroke, *Introduction to Coherent Optics and Holography*, Academic, 1966.

- ¹⁶L. M. Soroko, *Usp. Fiz. Nauk* **90**, 3 (1966) [*Sov. Phys.-Usp.* **9**, 643 (1967)].
- ¹⁷H. C. Montgomery, *BST Journ.* **17**, 406 (1938).
- ¹⁸V. A. Zverev and E. F. Orlov, *PTÉ*, No. 1, 50 (1960).
- ¹⁹M. Born, R. Furth, and R. W. Pringle, *Nature* **156**, (No. 3973), 756 (1945); *YMH* **1** [3/4 (13/14)], 172 (1946).
- ²⁰V. A. Cherepanov, *Izv. Vuzov (Radiotekhnika)* **5**, 409 (1962).
- ²¹A. Lohmann, *Optik* **14**, 510 (1957).
- ²²V. A. Zverev, I. V. Mosalov, E. F. Orlov, and V. L. Sibiryakov, *PTÉ* No. 1, 110 (1962).
- ²³M. S. Uberoi, *Rev. Sci. Instr.* **33**, 314 (1962).
- ²⁴J. C. Vienot, *Optica Acta* **5** (hors. ser.) 279 (1958); *Proc. Phys. Soc. (London)* **72**, 661 (1958).
- ²⁵Aebischer-Neoschill, Gaultier du Marache, P. M. Duffieux, J. C. Vienot, and W. J. Obert, *Proc. Fifth Conf. of Internat. Commission on Optics*, v. 2, Stockholm, 1959, p. 113.
- ²⁶J. S. Wilczynski, *Proc. Phys. Soc. (London)* **77** (493), 17 (1961).
- ²⁷R. Drougard and J. S. Wilczynski, *JOSA* **55**, 1938 (1965).
- ²⁸P. Prat, *Optica, Acta* **13** (2), 73 (1966); *Compt. Rend.* **262**, SB-597 (1966).
- ²⁹G. G. Slyusarev and N. I. Kulikovskaya, *Opt. spektrosk* **4**, 486 (1958).
- ³⁰G. Lansraux, *Rev. d'Optique* **32** (8/9) 475 (1953).

Translated by J. G. Adashko